Chapter 6
Mixer Reliability

Recently, active switching mixer design is widely used in CMOS millimeter-wave circuit design. Increasing demands for high speed and low cost home entertainment, imaging, and automotive radar systems lead to CMOS circuit and system research in millimeter-wave application. Some applications, such as HDMI wireless video receivers and point-to-point radio strongly require CMOS millimeter-wave devices to further implement SoCs [1]. The Gilbert cell structure has better isolation, conversion gain (CG), linearity, and compact size [2]. A double balanced Gilbert cell structure with Marchand baluns for broadband using TSMC 65 nm 1P6 M CMOS process was fabricated for the evaluation of mixer reliability. The Marchand balun provides simple structure, low amplitude/phase imbalance, and wideband frequency response [3, 4]. The stacked coupled balun is used for broadband matching and balance converting.

Figure 6.1 shows the simplified schematic of the double balanced mixer that consists of Marchand baluns for RF/LO input to obtain a wider range of bandwidth matching. The Marchand balun uses stacked coupled structure with top metal layer metal 6 (*M*6) and to metal 4 (*M*4). The response frequency is dominated by the length of the transmission line [5, 6]. The length of the transmission line is $\sim$1056 μm and the line width is 12 μm for *M*4 and 3 μm for *M*6. It has a wide matching bandwidth from 60 to 86 GHz for the RF port and 58.8–83.2 GHz for LO port. In our mixer design, the RF and LO ports use the transmission line matching network. C_1, C_2, $TL_{11,12}$, $TL_{21,22}$ are the matching network for the internal stage of transconductance stage (M_1 and M_2), while C_3, C_4, $TL_{31,32}$, $TL_{41,42}$ are for the switching stage ($M_{3,4}$ and $M_{5,6}$). TL_{51} and TL_{52} are transmission lines of the width 3 μm and length 100 μm for source degeneration to enhance internal stage matching bandwidth [7]. TL_{61} and TL_{62} are matching components between the transconductance and switching stages to improve the conversion gain of the mixer. R_1 and R_2 are resistive loads and equal to 175 Ω for optimal conversion gain. The conversion gain of the mixer is designed to work with 7 dBm LO power at 68 GHz. The LO input power is between 4–7 dBm from 64 to 75 GHz. Since the balun insertion loss is about 6 dB, the actual power to the LO transistors reduces to −2 to 2 dBm.

J.-S. Yuan, *CMOS RF Circuit Design for Reliability and Variability*,
SpringerBriefs in Reliability, DOI 10.1007/978-981-10-0884-9_6

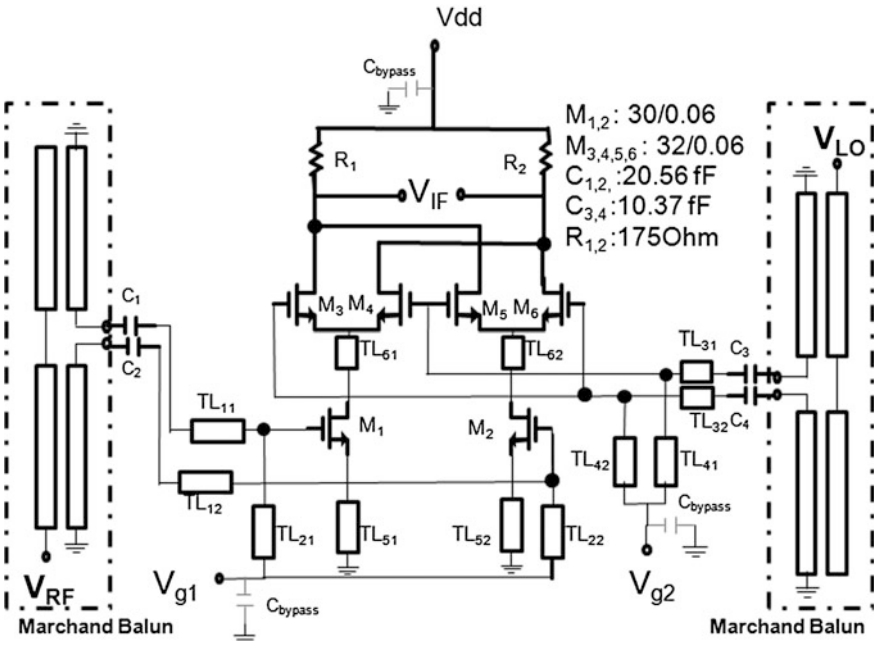

Fig. 6.1 Schematic of the down-converter mixer using Marchand baluns at RF/LO inputs

Fig. 6.2 Photograph of the down-conversion mixer

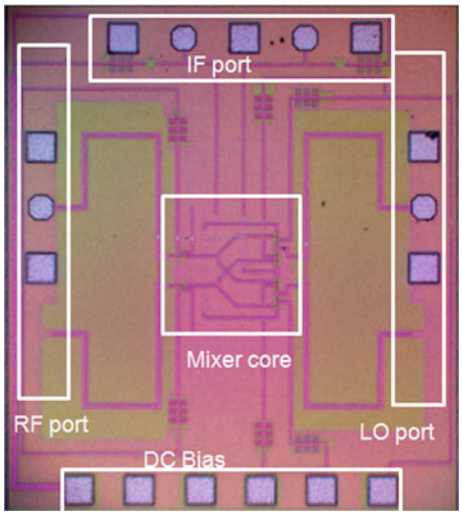

Figure 6.2 shows the die photograph of the fabricated millimeter-wave mixer using 65 nm 1P6 M CMOS technology. The chip size is 0.606 mm^2. A RF port (GSG) pad is on the left side and LO port (GSG) on the right. The top side is

balanced IF output (GS^+GS^-G). The DC pad is arranged in the order of V_{DD}, Gnd, V_{G1}, V_{G2}, Gnd, and V_{G2}.

Figure 6.3 shows measured input reflection coefficient of RF and LO ports at room temperature. The input stages of RF and LO transistors have a wide bandwidth matching from 60 to 86 GHz and 58.8–83.2 GHz for −10 dB reflection coefficient. The DC gate biasing for this measurement is under V_{G1} = 0.7 V and V_{G2} = 0.8 V. Figure 6.4 displays the measured isolation of the double balanced mixer LO-to-RF, LO-to-IF, and RF-to-IF from 60 to 85 GHz, where the isolation is less than −30 dB. The conversion gain performance of 68 GHz down-convert to f_{IF} at 1 GHz. Figure 6.5 shows the conversion gain versus the RF input power and the IF output power versus the LO input power. In Fig. 6.5, the solid squares represent

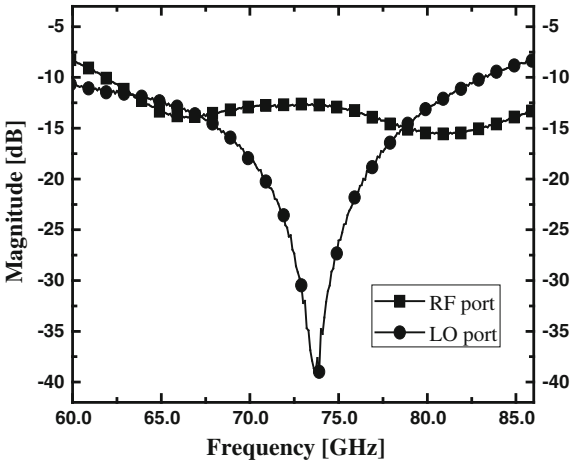

Fig. 6.3 Input reflection coefficient of input matching characteristics for RF and LO port

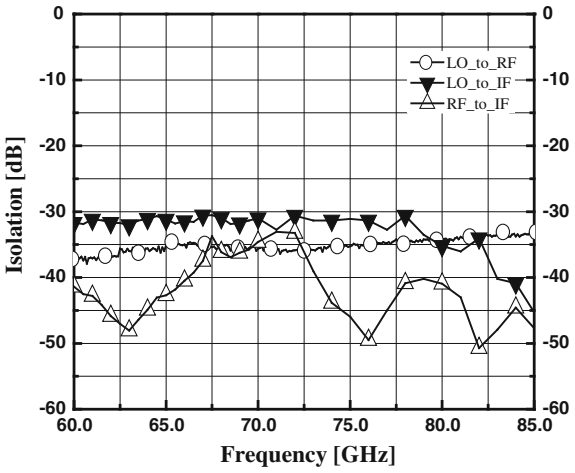

Fig. 6.4 Measured LO-to-RF, LO-to-IF, and RF-to-IF isolation verse RF frequency

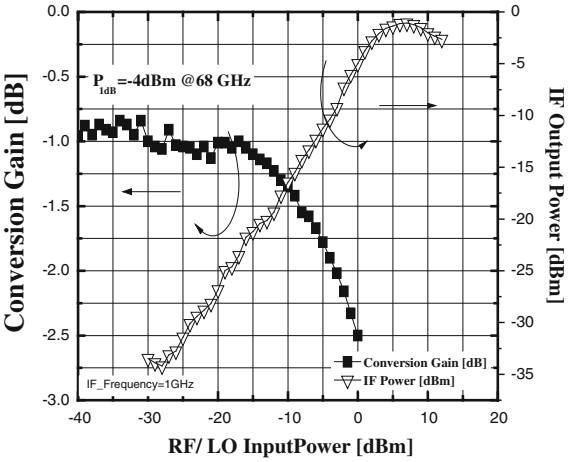

Fig. 6.5 Measured conversion gain versus RF/LO input power to illustrate input compression point (P1 dB) with RF of 68 GHz, a fixed IF frequency of 1 GHz

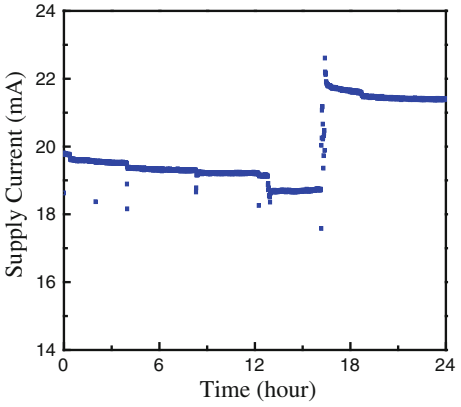

Fig. 6.6 Experimental data to the current from V_{DD} (the overstress voltage is @ V_{DD} = 2.5 V)

the conversion gain and the inverse triangle symbols represent the IF output power. As seen in Fig. 6.5, the saturation conversion gain is −0.93 dB. The corresponding IF output power at the 1 dB compression point (IP_{1dB}) is −4 dBm at 68 GHz.

RF stress experiment was performed under an elevated DC supply voltage V_{DD} of 2.5 V at room temperature. Figure 6.6 shows the measured mixer supply current from V_{DD} versus time. As seen in Fig. 6.6, the mixer supply current decreases with time in the beginning and then increases sharply, indicating oxide breakdown after about 17 h of dynamic stress at millimeter-wave frequency. The decrease in supply current in early 17 h is due to hot electron degradation that increases the threshold voltage and decreases the drain current of n-channel transistors of the mixer.

Figure 6.7 shows the mixer conversion gain versus RF frequency after different stress times. The conversion gain increases with RF frequency, but decreases with stress times, as expected. After 24 h of accelerated stress, the conversion gain can drop about 4 dB due to hot electron and oxide breakdown stress effects. At high RF

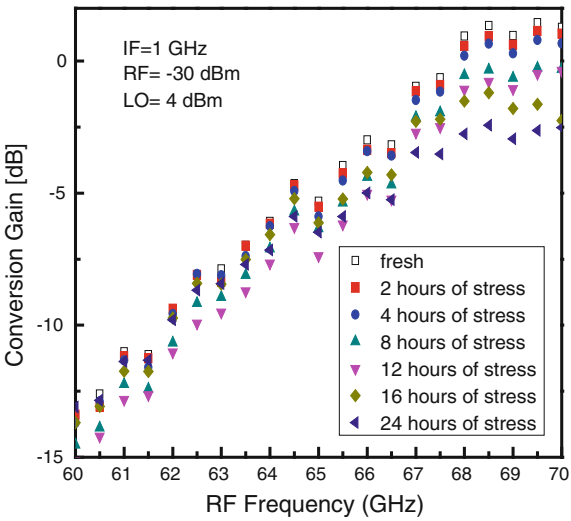

Fig. 6.7 Conversion gain versus RF frequency after different stress times

input power level, the conversion gain decreases with RF input power. The conversion gain also decreases with stress times at high RF input power at high RF input power, as observed by the measurement data in Fig. 6.7.

References

1. Cabric D, Chen M, Sobel D, Yang J, Broderson RW (2005) Future wireless systems: UWB, 60 GHz and cognitive radios. In: IEEE Custom Integrated Circuits Conference, 2005, pp 793–796
2. Mitomo T, Ono N, Hoshino H, Yoshihara Y, Watanabe I, Seto I (2010) A 77 GHz 90 nm CMOS transceiver for FMCW radar applications. IEEE J Solid-State Circuits 928–937
3. Sun J-T, He S-H, Liu Q, Liu H-W, Yoshimasu T (2011) Compact broadband Marchand balun with excellent imbalance performance for Si-based millimeter wave IC applications. In: China-Japan joint microwave conference proceedings (CJMW), 2011, pp 1–4, 20–22
4. Chiang M-J, Wu H-S, Tzuang C-K (2009) A compact CMOS Marchand balun incorporating meandered multilayer edge-coupled transmission lines. In: IEEE international microwave symposium, 2009, pp 125–128
5. Zhang Z, Guo Y-X, Ong LC, Chia MY (2004) Improved planar marchand balun using a patterned ground plane. Wiley Periodicals, Inc. pp 307–316
6. Liu J-X, Hsu C-Y, Chuang H-R, Chen C-Y (2007) A 60-GHz Millimeter-wave CMOS Marchand Balun. In: IEEE radio frequency integrated circuits (RFIC) symposium, 2007, pp 445–448
7. Lerdworatawee J, Won N (2005) Wide-band CMOS cascode low-noise amplifier design based on source degeneration topology. In: IEEE Trans Circuits and Systems I: Regular Papers, pp 2327–2334